Freestanding Membranes of Cross-Linked Gold-Nanoparticles: Novel Functional Materials for MEMS/NEMS Applications

H. Schlicke*, C. J. Schröter*, M. Rebber*, D. Battista*, S. Kunze* and T. Vossmeyer*

* Institute of Physical Chemistry, University of Hamburg,
Grindelallee 117, 20146 Hamburg, Germany
email: schlicke@chemie.uni-hamburg.de

ABSTRACT

3D cross-linking of gold-nanoparticles (GNPs) with alkylene dithiol molecules renders thin films with unique optical, mechanical and charge transport characteristics that can be tuned by variation of the GNP size and shape as well as by the nature of the dithiol molecule. So far, substrate-supported films were successfully applied as resistive strain gauges and chemiresistors. The films exhibit mechanical stability, sufficient to transfer and deposit them as freestanding membranes onto a variety of 3D structured substrates. The tunability of the material properties as well as the strain sensitivity make cross-linked GNP membranes interesting candidates for the implementation in micro- / nanoelectromechanical systems (MEMS/NEMS). Here, we report on the investigation of electromechanical properties of freestanding cross-linked GNP membranes and explore their applicability in MEMS/NEMS, i.e. as functional materials in pressure sensors or electrostatic actuators.

Keywords: gold, nanoparticle, MEMS, NEMS, membrane

1 INTRODUCTION

Recently, freestanding membranes of monothiol capped gold nanoparticle (GNP) monolayers[1, 2] as well as polymer-encapsulated GNPs[3] were fabricated and attracted interest due to their potential applications, e.g. as pressure sensors with optical readout or drumhead resonators using piezoelectric actuation. However, layers of GNPs capped with long-chain organic ligands or encapsulated in a polymer matrix commonly show low conductivity, due to the large tunneling gaps formed by the ligand shells seperating the nanoparticles. Conductive GNP films can be obtained by shrinking these gaps, i.e. by ligand exchange with short-chain ligands or cross-linkage of the GNPs using e.g. short dithiol molecules. The electrical conductivity of such GNP films can be well-described by a simple semiempirical Arrhenius-type activated tunneling model (equation 1).[4, 5]

$$\sigma = \sigma_0 e^{-\beta\delta} e^{-\frac{E_A}{kT}} \quad (1)$$

Here, σ_0 is a preexponential factor, β is the tunneling decay constant, δ denotes the interparticle distance, E_A the activation energy, T the temperature and k is the Boltzmann constant. As the conductivity strongly depends on the interparticle distance, it is highly sensitive to external stimuli. For example, upon application of strain to a conductive GNP composite, it is transferred to the flexible organic matrix leading to further seperation of the particles and hence a change in resistance. This lead to investigations of the applicability of substrate-supported GNP composite films as strain gauges.[6, 7, 8, 9] Gauge factors of up to 200 were measured.[6] Besides a high sensitivity to strain, the conductivity of GNP composites is influenced when exposing the material to chemical vapors or gases.[10, 11, 12, 9] This behavior is attributed to analyte uptake by the organic matrix, resulting in an increase of the interparticle distance due to swelling and changes in its dielectricity.[9] While extensive work was conducted investigating the above-mentioned characteristics of substrate-supported GNP composites, the investigation of electromechanical properties and potential applications of freestanding, conductive, cross-linked GNP composites is still in its infancy. The focus of our work is the investigation of these properties, e.g. by atomic force microscopy based micro bulge tests,[13] and the exploration of potential applications of the membranes in MEMS/NEMS.

2 FABRICATION OF GNP MEMBRANES

There are different methods reported for the fabrication of substrate-supported dithiol cross-linked gold nanoparticle composite films. Bethell et al.[14] reported on the fabrication of GNP/dithiol networks on functionalized SiO_2 surfaces. Firstly, the substrate surface was functionalized with mercaptosilanes. Upon immersion of the functionalized substrate into a solution of weakly capped gold colloids, the latter bound to the thiol groups exposed by the substrate. Afterwards, solutions of dithiols and gold colloids were applied alternately, leading to the successive formation of a GNP-dithiol network. Similar layer-by-layer self-assmebly (LBL-SA) processes were used by different groups to fabricate thin films con-

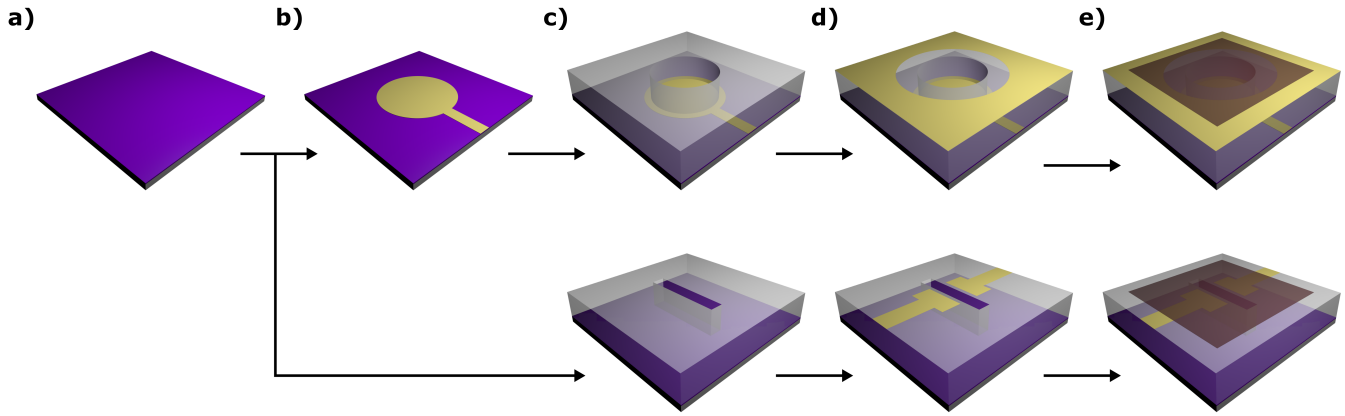

Figure 1: Fabrication process of different GNP-membrane based devices. The top row depicts the fabrication of an electrostatic actuator, while the bottom row depicts the fabrication process of a GNP membrane based ambient pressure sensor. *a)* A silicon wafer with a thermal oxide layer acts as substrate. *b)* If desired, Ti/Au back electrodes were deposited onto the substrate. *c)* SU-8 epoxy photoresist is used for fabricating 3D structures with cavities for freestanding membrane deposition. *d)* Deposition of Au top electrodes for electrically contacting the freestanding membranes. *e)* GNP membrane deposition.

sisting of GNP-dithiol networks on glass[5, 11] or polymer (polyethylene)[9, 7] substrates.

While these LBL-SA processes exhibit different advantages for the fabrication of substrate-supported GNP networks, e.g. a high degree of control and excellent particle cross-linking ratios,[11] they show major drawbacks when it comes to the fabrication of freestanding GNP membranes by lift-off and transfer procedures, as the resulting GNP networks are covalently attached to the substrate. For the fabrication of GNP membranes we follow a procedure which was published by our group in 2011.[15]

Here, a solution of GNPs with weakly bound dodecylamine (DA) ligands in heptane was spin-coated onto glass substrates. Subsequently, a methanolic solution of an alkylene dithiol was spin-coated leading to a ligand exchange and formation of a thin film of cross-linked GNPs. The two deposition steps could be repeated to obtain GNP-dithiol composite films with controlled thickness in the $20 - 100\,\mathrm{nm}$ range. Compared to the conventional self-assembly based processes, the spin-coating based deposition enables rapid fabrication of the thin films and - due to the absence of strong chemical binding between the film and the substrate - a lift-off of the film. This can be achieved either by alkaline underetching[16, 15] or careful immersion of the substrates into deionized water,[17] leading to detachment of the film, which then remains floating at the liquid-air interface and can be transferred to arbitrary substrates.

3 DEVICE FABRICATION AND CHARACTERIZATION

Different microstructures were used as support for the freestanding GNP membranes, depending on the target application of the final device. In this paper, we present the exploration of two different MEMS applications of dithiol cross-linked GNP membranes. On the one hand, we demonstrated the fabrication of a resistive ambient pressure sensor, employing a GNP membrane as strain sensitive transducer.[18] On the other hand, we demonstrated electrostatic actuation of freestanding GNP composite membranes.[17] These two applications will be discussed in the following. The fabrication of the devices was similar in both cases. Figure 1, top row, schematically depicts the fabrication process of an electrostatic actuator device, while the fabrication of an ambient pressure sensor is depicted in the bottom row. Commonly, 3D microstructures were fabricated onto doped silicon wafers with thermally grown oxide layers, acting as insulation barriers.

3.1 Ambient Pressure Sensor

In a recent paper, we demonstrated the applicability of dithiol cross-linked GNP membranes as strain sensitive transducers in resistive ambient pressure sensors.[18] The fabrication of such a device is schematically depicted in figure 1, bottom row. Onto a silicon wafer substrate, a layer of SU-8 photoresist was deposited and a microcavity was subsequently fabricated using photolithography. On top of this relief structure, following a lift-off procedure, gold electrodes were deposited in proximity to the cavity. Finally, a 1,6-hexanedithiol

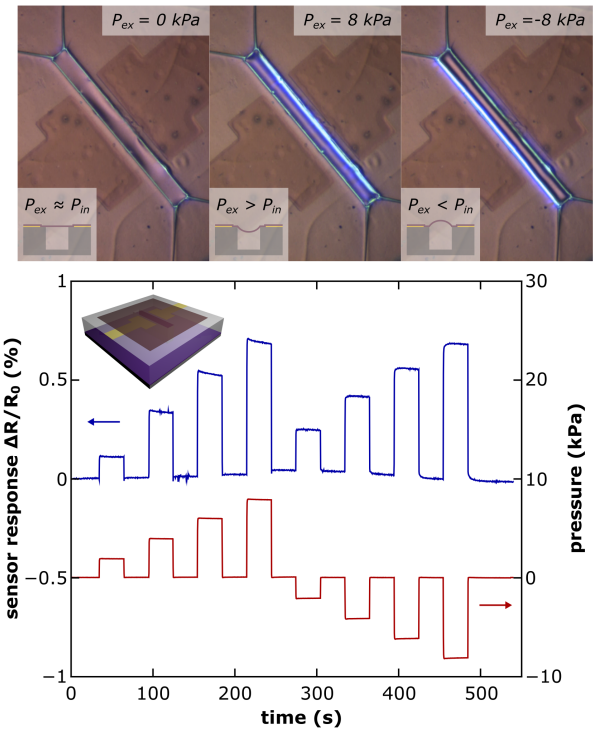

Figure 2: *(top)* Micrographs of a GNP membrane based resistive pressure sensor upon application of different external pressures. The device comprises a 55 nm thick 6DT cross-linked GNP membrane, sealing a $\sim 40\,\mu$m wide and $\sim 40\,\mu$m deep microcavity. *(bottom)* Time trace of the GNP membrane pressure sensor response *(upper blue line)* to applied external pressure transients *(lower red line)*. The resistance was read out by electrodes deposited in proximity to the cavity. Adapted from Ref. [18] with permission from The Royal Society of Chemistry.

(6DT) cross-linked GNP membrane was transferred to the microstructure, as described above.

In this type of pressure sensor, the GNP membrane acts both as diaphragm, and as strain sensitive transducer. Sealing the microcavitiy, the membrane deflects upon variation of the external pressure, due to the pressure difference between the cavity volume and the exterior. The resulting strain causes a change in the membrane's resistance that can simply be read out by contacting the electrodes in proximity to the microcavity.

For characterization the devices were placed in a pressure cell, suitable to apply positive and negative pressures (relative to ambient) in a range of ± 10 kPa. The cell pressure as well as the resistance of the device were constantly monitored using digital reference pressure gauges (Sensortechnics) and a Keithley 2601A source measure unit. Figure 2 shows an exemplary resistance and pressure trace, recorded while applying pressures in a range from approximately -8 to 8 kPa to a device comprising a 55 nm thin 6DT cross-linked GNP membrane, placed onto a $\sim 40\,\mu$m wide microcavity (depth $\sim 40\,\mu$m). Upon application of positive and negative pressures up to $|P| \sim 8$ kPa (relative to ambient), deflections of the membrane (see figure 2, top) and a resistance change up to $\sim 0.7\%$ were observed. As expected, the sensor response was nearly independent of the applied pressure's direction. The transfer function of the device was further analyzed and could be well-described using a simple theoretical model.[18]

3.2 Electrostatic Actuator

Further, we demonstrated electrostatic actuation, a widely used principle in MEMS/NEMS, of freestanding, dithiol cross-linked GNP membranes.[17] The fabrication of electrostatic membrane actuators is depicted in figure 1, top row. Again, doped silicon wafers with thermally grown oxide layers were used as substrates. While the wafers could either be used as global counter electrodes themselves, alternatively, structured Ti/Au back electrodes were fabricated for addressing different actuators on one wafer substrate individually. On top of the back electrode structure a layer of SU-8 was deposited and structured using photolithography to yield microcavities of a desired shape. Subsequently, a structured gold top electrode, suitable for contacting a GNP membrane and used as signal ground, was deposited on top of the SU-8 layer. Finally, a 6DT cross-linked GNP membrane was transferred to the 3D electrode structure following the lift-off and transfer process described above. The membrane settled to the electrode structure and remained freestanding on the microcavity.

To demonstrate electrostatic actuation of freestanding, 6DT cross-linked GNP membranes, DC voltages were applied between the top and back electrodes. The potential difference resulted in coulomb forces, pulling the freestanding membrane into the SU-8 cavity. Deflections of the membranes were monitored using atomic force microscopy, confocal microscopy and laser interferometry.[17] Figure 3 depicts exemplary data measured investigating a 6DT cross-linked GNP membrane (thickness 46 nm) deposited onto a $\sim 150\,\mu$m diameter circular SU-8 cavity, $\sim 8\,\mu$m above the back electrode. Voltage transients up to ± 40 V were applied between the membrane and the back electrode and deflections up to $\sim 0.8\,\mu$m were observed using laser interferometry (SIOS Nanovibration Analyzer NA). The voltage-deflection behavior of different devices was measured and approximated using a theoretical model.[17]

The results demonstrate that electrostatic actuation can be used for excitation of freestanding GNP membranes, which is an important step towards the fabrication of more advanced devices, such as electrostatically driven membrane resonators.

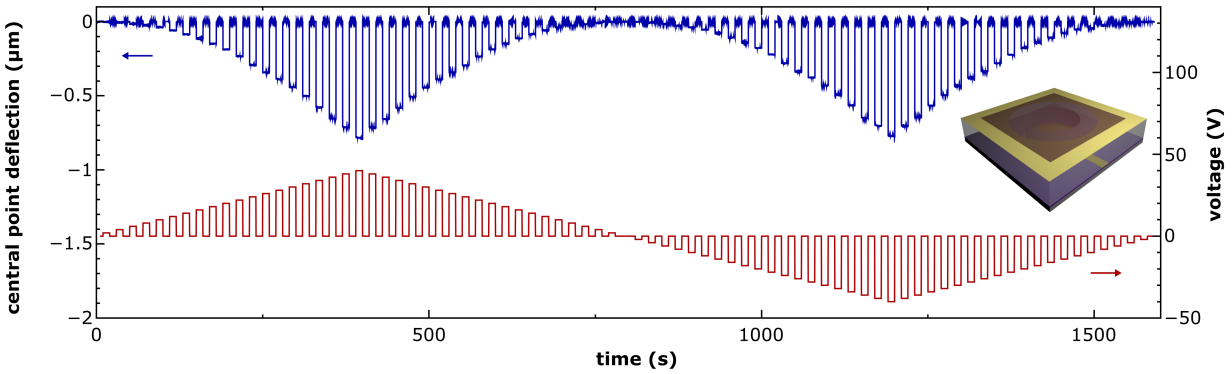

Figure 3: Deflection time trace *(upper blue line)* of a GNP membrane based electrostatic actuator upon application of voltage transients in a range of ±40 V *(lower red line)*. The device comprised a 46 nm thick 6DT cross-linked GNP membrane, deposited onto a ∼ 150 µm diameter circular microcavity, ∼ 8 µm above a back electrode. Deflections were measured in the center of the membrane using laser interferometry and corrected for a drift caused by the measurement setup.

4 SUMMARY

In summary, our results underline that freestanding conductive membranes of cross-linked gold nanoparticles are interesting candidates for the fabrication of MEMS/NEMS. The applicability of the composite material as strain sensitive transducer in resistive pressure sensors was demonstrated and electrostatic actuation of the membranes was shown. Current studies aim at the fabrication of electrostatically driven GNP membrane drumhead resonators for microgravimetric or pressure sensing applications.

5 ACKNOWLEDGEMENTS

The work of H.S. is supported by a scholarship of the Joachim Herz Stiftung. T.V. acknowledges financial support by the DFG, grant number VO698/3-1.

REFERENCES

[1] Mueggenburg, K. E.; Lin, X.-M.; Goldsmith, R. H.; Jaeger, H. M. *Nat. Mater.* **2007**, *6*, 656–660.

[2] Kanjanaboos, P.; Lin, X.-M.; Sader, J. E.; Rupich, S. M.; Jaeger, H. M.; Guest, J. R. *Nano Lett.* **2013**, *13*, 2158–62.

[3] Jiang, C.; Markutsya, S.; Pikus, Y.; Tsukruk, V. V. *Nat. Mater.* **2004**, *3*, 721–728.

[4] Terrill, R. H.; Postlethwaite, T. A.; Chen, C.-h.; Poon, C.-D.; Terzis, A.; Chen, A.; Hutchison, J. E.; Clark, M. R.; Wignall, G.; Londono, J. D.; Superfine, R.; Falvo, M.; Johnson Jr., C. S.; Samulski, E. T.; Murray, R. W. *J. Am. Chem. Soc.* **1995**, *117*, 12537–12548.

[5] Wessels, J. M.; Nothofer, H.-G.; Ford, W. E.; von Wrochem, F.; Scholz, F.; Vossmeyer, T.; Schroedter, A.; Weller, H.; Yasuda, A. *J. Am. Chem. Soc.* **2004**, *126*, 3349–3356.

[6] Herrmann, J.; Müller, K.-H.; Reda, T.; Baxter, G. R.; Raguse, B.; de Groot, G. J. J. B.; Chai, R.; Roberts, M.; Wieczorek, L. *Appl. Phys. Lett.* **2007**, *91*, 183105.

[7] Vossmeyer, T.; Stolte, C.; Ijeh, M.; Kornowski, A.; Weller, H. *Adv. Funct. Mater.* **2008**, *18*, 1611–1616.

[8] Farcau, C.; Moreira, H.; Viallet, B.; Grisolia, J.; Ciuculescu-Pradines, D.; Amiens, C.; Ressier, L. *J. Phys. Chem. C* **2011**, *115*, 14494–14499.

[9] Olichwer, N.; Leib, E. W.; Halfar, A. H.; Petrov, A.; Vossmeyer, T. *ACS Appl. Mater. Interfaces* **2012**, *4*, 6151–6161.

[10] Wohltjen, H.; Snow, A. W. *Anal. Chem.* **1998**, *70*, 2856–2859.

[11] Joseph, Y.; Besnard, I.; Rosenberger, M.; Guse, B.; Nothofer, H.-G.; Wessels, J. M.; Wild, U.; Knop-Gericke, A.; Su, D.; Schlögl, R.; Yasuda, A.; Vossmeyer, T. *J. Phys. Chem. B* **2003**, *107*, 7406–7413.

[12] Ibañez, F. J.; Zamborini, F. P. *Small* **2011**, *8*, 174–202.

[13] Schlicke, H.; Leib, E. W.; Petrov, A.; Schröder, J. H.; Vossmeyer, T. *J. Phys. Chem. C* **2014**, *118*, 4386–4395.

[14] Bethell, D.; Brust, M.; Schiffrin, D. J.; Kiely, C. *J. Electroanal. Chem.* **1996**, *409*, 137–143.

[15] Schlicke, H.; Schröder, J. H.; Trebbin, M.; Petrov, A.; Ijeh, M.; Weller, H.; Vossmeyer, T. *Nanotechnology* **2011**, *22*, 305303.

[16] Kowalczyk, B.; Apodaca, M. M.; Nakanishi, H.; Smoukov, S. K.; Grzybowski, B. A. *Small* **2009**, *5*, 1970–1973.

[17] Schlicke, H.; Battista, D.; Kunze, S.; Schröter, C. J.; Eich, M.; Vossmeyer, T. *ACS Appl. Mater. Interfaces* **2015**, *7*, 15123–15128.

[18] Schlicke, H.; Rebber, M.; Kunze, S.; Vossmeyer, T. *Nanoscale* **2016**, *8*, 183–186.